

Review

Clinical Applications of Optical Coherence Angiography Imaging in Ocular Vascular Diseases

Claire L. Wong¹, Marcus Ang^{1,2,3} and Anna C. S. Tan^{1,2,3,*}

¹ Singapore National Eye Centre, Singapore 168751, Singapore; claire.wong@mohh.com.sg (C.L.W.); marcus.ang@singhealth.com.sg (M.A.)

² Singapore Eye Research Institute, Singapore 169856, Singapore

³ Ophthalmology and Visual Sciences, Duke-National University of Singapore, Singapore 169857, Singapore

* Correspondence: anna.tan.c.s@singhealth.com.sg

Received: 14 May 2019; Accepted: 19 June 2019; Published: 25 June 2019



Abstract: Optical coherence tomography angiography (OCTA) provides us with a non-invasive and efficient means of imaging anterior and posterior segment vasculature in the eye. OCTA has been shown to be effective in imaging diseases such as diabetic retinopathy; retinal vein occlusions; retinal artery occlusions; ocular ischemic syndrome; and neovascularization of the iris. It is especially useful with depth-resolved imaging of the superficial, intermediate, and deep capillary plexi in the retina, which enables us to study and closely monitor disease progression and response to treatment. With further advances in technology, OCTA has the potential to become a more widely used tool in the clinical setting and may even supersede ocular angiography in some areas.

Keywords: optical coherence tomography angiography; diabetic retinopathy; retinal vein occlusion; retinal artery occlusion; ocular ischemic syndrome; neovascularization; iris neovascularization

1. Introduction

Optical coherence tomography technology has developed rapidly over the past decade [1]. The advent of ocular coherence tomography angiography (OCTA) in recent years has provided clinicians and scientists with a non-invasive and quick method of obtaining ocular angiographic images of vascular structures [2]. OCTA has been widely employed in studying a host of posterior segment pathology such as diabetic retinopathy, retina vein occlusions, retina artery occlusions, choroidal neovascularization, and optic neuropathies [3,4]. OCTA technology has also been adapted for anterior segment imaging [1], and has been useful in imaging iris, cornea, and anterior segment vessels [5,6].

OCTA allows for visualization of functional blood vessels by using the flow of red blood cells as intrinsic contrast agents [7]. Decorrelation signals, which are differences in backscattered OCT signal intensity and amplitudes between consecutive scans, are compared using OCTA algorithms that employ phase-signal-based, intensity-signal-based, and complex-signal-based techniques [1,3,8]. The system then generates depth-resolved ‘flow’ images and three-dimensional en face structural sections, which can be viewed together in a dynamic fashion [9,10]. Rapid acquisition and the generation of angiographic images is possible and with no requirement of dye injections, which can pose associated risks. In comparison to conventional dye angiography such as fundus fluorescein angiography (FA) and indocyanine green angiography (ICG), OCTA can simultaneously image both retinal and choroidal microvasculature and due to the depth resolution, the visualization of superficial, intermediate, and deep capillary networks can be distinguished and delineation of vascular lesions within the retinal layers can be imaged in a three-dimensional manner [3,7].

Currently, fundus fluorescein angiography (FA) and indocyanine green angiography (ICG) are the gold standard for imaging vasculature in the posterior segment and have been widely used in

ophthalmology for decades. Current commercially available angiography platforms have the potential to provide a wide field of view and dynamic visualization of blood flow. Leakage of fluid or blood can be observed as hyperfluorescence and may be useful to help monitor disease progression and response to therapy associated with various vascular pathologies [3]. ICG can also be used to assess anterior segment vasculature and is effective where there is inadequate vessel delineation on slit lamp photography [11]. However, both of these methods are invasive, expensive, and time-consuming. The dye used also poses risk of allergy and ICG is contraindicated in pregnancy and kidney disease. Two types of dye are also required to image both retina and choroidal vessels. As the image obtained is two-dimensional, lesions observed are not depth-resolved. Also, while leakage provides useful information, in some chronic, extensive retinal and choroidal diseases, the leakage may not be able to be distinguished clearly or be obscured by blood making the diagnosis ambiguous [3,4,7,12]. Furthermore, leakage of vascular lesions in conventional angiography may differ depending on the exact stage when the lesion is imaged. This makes it challenging to quantify the actual vascular pathology during disease progression [7].

Chronic systemic vascular diseases such as diabetes mellitus, hypertension, and hyperlipidemia are an increasing burden on healthcare worldwide [13]. These are risk factors for developing ocular vascular diseases, which are often sight-threatening [14–16]. This review will focus on the clinical applications of anterior and posterior segment OCTA in the diagnosis and disease monitoring of diabetic retinopathy (DR), retinal vein occlusion (RVO), retinal artery occlusion (RAO), and ocular ischemic syndrome (OIS).

2. Diabetic Retinopathy

Diabetic retinopathy is one of the World Health Organization's priority eye diseases [17]. DR is a leading cause of visual impairment in working-age adults in most developed countries. Early detection of retinopathy is critical in preventing vision loss [18]. In diabetes, the hyperglycemic state damages small retinal vessels, retinal cells, and components of the blood-retina-barrier. The damage manifests as microaneurysms, intraretinal hemorrhages, intraretinal microvascular abnormalities, venous beading, cotton wool spots, hard exudates, intraretinal cysts, subretinal fluid, and neovascularization (Figures 1A and 3A) [14,19]. Sight-threatening complications of diabetes include diabetic macular edema (DME), macular ischemia, and proliferative disease associated with vitreous hemorrhage, traction retinal detachments, and neovascular glaucoma [20,21].

2.1. Role of FA in Diabetic Retinopathy

FA has been the imaging modality of choice for diagnosis and monitoring in DR. Investigators from the Early Treatment Diabetic Retinopathy Study (ETDRS) have historically classified diabetic retinopathy using FA [22,23]. Their protocol consists of stereoscopic FA of two 30-degree fields extending horizontally from 25 degrees nasal to the disc to 20 degrees temporal to the macula. The foveal avascular zone (FAZ), capillary loss, capillary dilatation, arteriolar, and retinal pigment epithelium abnormalities are assessed in the early-mid phase of the FA and fluorescein leakage, source of leakage and cystoid changes are graded in the late phase [23]. These FA findings are also compared to standard reference photographs [23].

Recent improvements in FA imaging include ultra-wide-field imaging and video angiography. However as mentioned above, FA is time-consuming and has drawbacks. In addition, FA is not depth-resolved and hence is unable to differentiate the superficial, intermediate, and deep capillary plexi of the retina well [4,12].

2.2. Role of OCTA in Diabetic Retinopathy

Diabetic retinopathy profoundly affects retinal vasculature and OCTA allows depth-resolved, high-resolution imaging that has enabled the improved identification of many detailed pathological features in the superficial, intermediate, and deep vascular plexuses [12,24]. Features that can be

identified on OCTA include capillary dropout, vessel tortuosity, vascular remodeling, choriocapillaris abnormalities, areas of non-perfusion, intraretinal microvascular abnormalities, and disc, retinal, and iris neovascularization [25,26].

2.2.1. OCTA for Non-Proliferative Diabetic Retinopathy

The role of OCTA has been extremely useful, especially in imaging the milder stages of diabetic retinopathy where FA may not be indicated. Studies have shown that OCTA can detect retinal vascular abnormalities including the location of microaneurysms, capillary non-perfusion, changes in the FAZ, alterations in the deep retinal layer, and impairment in the choriocapillaris before clinically detectable disease occurs [26–28]. Salz et al. showed that ultra-high-speed swept source OCTA was able to identify the majority of microaneurysms noted on FA and localize the microaneurysms to a specific vascular plexus using en face depth-resolved imaging [29]. Matsunga et al. also found that microaneurysms take on different shapes on OCTA despite their similar appearance as round dots on FA [30].

The deep capillary plexus (DCP) has been demonstrated to be more severely affected in diabetes compared to the intermediate (MCP) and superficial plexuses (SCP) [31]. Recently, Rodrigues et al. showed that the parafoveal vessel density in the DCP was the parameter that was most closely associated with ETDRS grading [32]. Another study showed that the 3 × 3-mm SCP and the DCP vessel density were the most accurate parameters for the detection of high-risk DR [33]. Using a statistical model, another study identified the superficial capillary plexi of the FAZ area, DCP vessel density, and acircularity as parameters that best distinguished between DR severity groups [34]. Increasing interest in the MCP has shown that both the MCP and DCP show parallel changes to DR progression. Therefore, including the MCP within the SCP may cause confounding results [35]. However, the automated quantification of MCP is not widely available on commercial OCTA platforms at present.

2.2.2. OCTA for Proliferative Diabetic Retinopathy

The main role of OCTA in the diagnosis and monitoring of proliferative diabetic retinopathy includes the detection of neovascularization. On cross-sectional OCTA, neovascularization appears as a positive flow signal extending from the retinal surface into the vitreous (Figure 1—yellow circle) [36]. Hwang et al. demonstrated that segmenting flow signal at the inner boundary of the superficial plexus, which is the internal limiting membrane, and projecting the signal in cross-sectional orientation enables visualization of vertical neovascularization. The flow signals are seen as shadows as they are elevated out of the depth range of OCTA [37]. This differs from intra-retinal microvascular abnormalities, which are confined to the retinal layers [36]. Areas of neovascularization can be clearly identified on consecutive OCTA imaging as margins are not obscured by leakage. This allows “sentinel” neovascular lesions to be closely monitored for regression in response to therapy with pan-retinal photocoagulation or intravitreal anti-vascular growth factor injections (Figure 2—yellow and green circles) [4,36]. A recent study used both cross-sectional OCT and OCTA to show that active neovascularization can be differentiated from fibrovascular tufts and proliferation into the vitreous by the presence of flow signals. On the en face OCTA, active neovascularization was seen as vascular tufts and regressed neovascularization in response to injections were visualized as ghost vessels or pruned vascular loops [36].

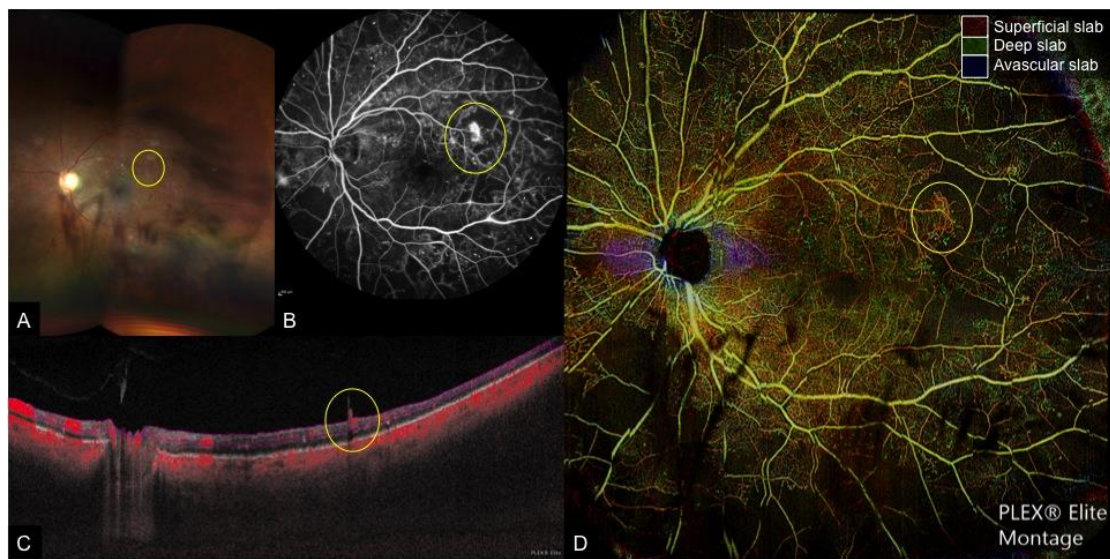


Figure 1. Multi-modal imaging of a case of proliferative diabetic retinopathy and vitreous hemorrhage. (A): Wide-field fundus photograph depicting scattered retinal hemorrhages with vitreous hemorrhage obscuring the temporal and inferior view of the retina, (B): Fundus fluorescein angiography (FA), (C): Cross-sectional optical coherence tomography angiography (OCTA) with flow indicated in red, and (D): Color-coded depth-resolved en face OCTA montage, which is a fusion image of the superficial (red), deep (green), and avascular (blue) en face OCTA slabs. New vessels (yellow circle) are seen on FA as areas of leakage and on cross-sectional OCTA as areas of flow extending from the retinal surface into the vitreous, which corresponds to fronds of vessels on en face OCTA.

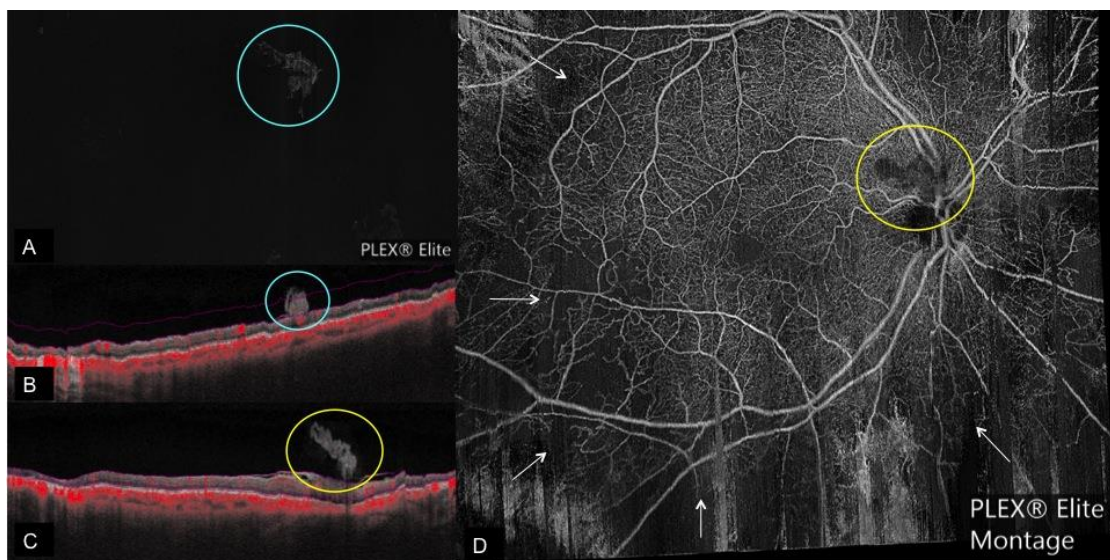


Figure 2. Regressed neovascularization on OCTA. (A): Regressed neovascular lesion (blue circle) seen on vitreous segmentation on en face OCTA with the corresponding cross-sectional OCTA. (B) Showing the regressed neovascular lesion with patchy area of flow (indicated by red color) extending from the retina surface into the vitreous; pink lines on B depict the boundaries of vitreous segmentation; (C): Cross-sectional OCTA image of a regressed neovascular lesion of the disc with no flow (yellow circle) corresponding to the en-face OCTA Montage; (D): Showing the regressed neovascularization of the disc with no flow (yellow circle) and flow voids (white arrows) after panretinal photocoagulation.

The efficiency and ease of OCTA imaging allows consecutive imaging to be performed at every follow-up visit, which was previously not possible with conventional angiography [38]. Hence, parameters such as macula vessel density and FAZ can be closely monitored. These parameters

have been shown to be early predictors of DR and correlate to DR severity and visual function, with the FAZ enlarging with progression of DR [4,29,39]. Agemy et al. found a significant decrease in capillary perfusion density in nearly all retina layers of diabetic patients compared with controls. This decrease in perfusion density worsened according to disease severity [40]. Looping vessels on OCTA adjacent to areas of impaired capillary perfusion have also been demonstrated to be consistent with intraretinal microvascular abnormalities. Of note, these are not visualized in areas with good capillary perfusion (Figure 3—yellow circles) [30]. A recent study using 12 mm × 12 mm widefield OCTA imaging showed that extra-macula areas had higher rates of non-perfusion compared to the macula area. Macula non-perfusion was also higher in eyes with proliferative diabetic retinopathy than severe non-proliferative diabetic retinopathy; no such difference was found in the extra-macula areas. They proposed that large arterioles residing in the SCP and DCP may act as perfusion boundaries. In the macula, overlapping feeding arterioles joined by the DCP may act as collateral vessels, which may reduce the probability of non-perfusion but be more susceptible to damage in proliferative disease [41].

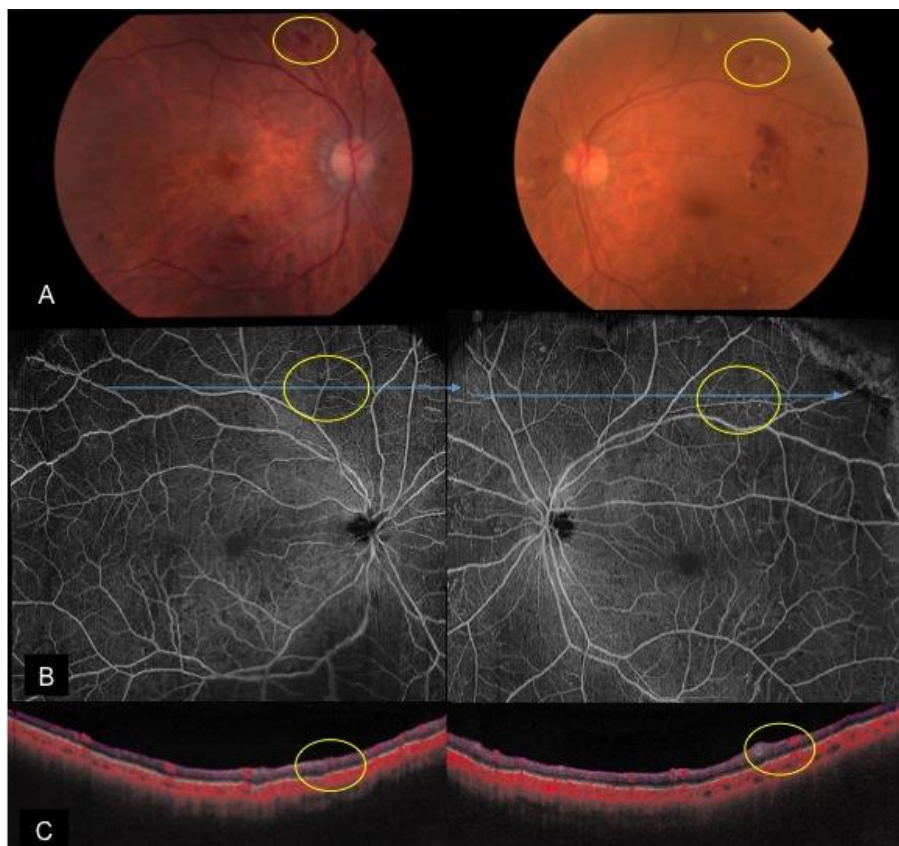


Figure 3. A case of bilateral severe non-proliferative diabetic retinopathy with intraretinal microvascular abnormalities. (A): Color fundus photos depicting scattered retinal hemorrhages and cotton wool spots; en face OCTA montage (B) and cross-sectional OCTA (C) reveal intraretinal microvascular abnormalities (yellow circles) in areas with slightly decreased capillary perfusion.

Diabetic macular ischemia at the level of the DCP has been shown to be associated with outer retinal disruption, which correlates to losses in visual function [31]. OCTA is useful for detecting and monitoring the progression of macular ischemia [14]. OCTA is especially helpful for explaining visual loss in patients with normal retina structure and for predicting long-term visual prognosis [38]. A pre-operative OCTA to assess a patient with diabetic retinopathy who is undergoing cataract surgery may be useful for pre-operative counselling and predicting post-operative visual prognosis.

2.2.3. OCTA for Diabetic Macular Edema

OCTA imaging in eyes with DME allows for comparison of changes in capillary density, dropout, and to study flow signals in relation to intraretinal cystic spaces caused by capillary leakage. Hasegawa et al. also showed that most microaneurysms are found in the deep capillary layer and in areas with DME [42]. However, in the presence of severe DME, anatomical distortion of the retinal layers makes accurate segmentation of the SCP and DCP challenging. Cystoid spaces can be differentiated from areas of non-perfusion by their shape and through comparison on structural and en face images. In DME, cystoid spaces are surrounded by areas of capillary dropout on OCTA. Mané et al. showed disruption of the deep plexus pattern in DME and that the deep capillary plexus is more involved than the superficial capillary plexus. In addition, they found and that no reperfusion occurred in areas of cystoid spaces after resolution of DME [43]. Similarly, Moein et al. demonstrated that retinal ischemia and loss of normal vasculature contributes to disorganization of retinal inner layers after resolved DME [44].

3. Retina Vein Occlusion

In retinal vein occlusion (RVO), stagnation of blood flow in retinal venous occlusion causes elevated venous and tissue pressure, tissue hypoxia, and extravasation of blood constituents. Age, raised intraocular pressure, and systemic vascular risk factors such as hypertension, hyperlipidemia, diabetes, and smoking are common predisposing risk factors. There are three types of vein occlusions: central, branch, and hemi-retinal vein occlusion [45–47]. Clinically, retina vein occlusions usually begin at an arteriovenous crossing and are characterized by dilation and tortuosity of the affected venous segment, flame-shaped, dot and blot hemorrhages, retina edema, and cotton wool spots (Figure 4A). Macular edema and neovascularization are common complications that can develop [45]. Retinal vein occlusions have been previously divided into ischemic and non-ischemic forms with certain definitions [48]. However, the increasing use of anti-vascular endothelial growth factor injections for the treatment of macular edema impacts peripheral ischemia, making these definitions less clear during the course of treatment [49,50].

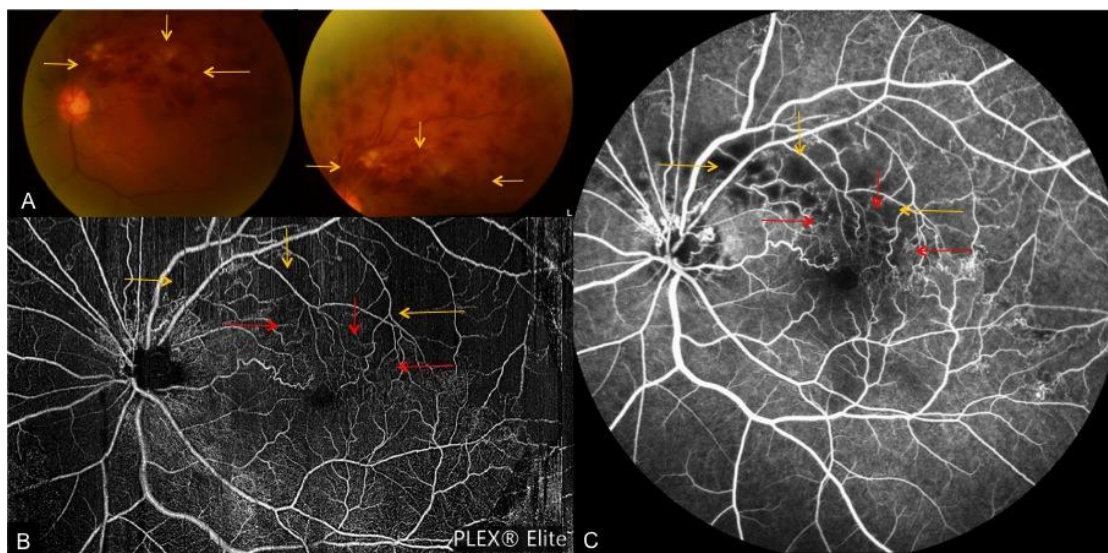


Figure 4. A case of fresh superior-temporal branch retinal vein occlusion. (A): Color fundus photos depicting tortuous venous segments with flame-shaped, dot and blot hemorrhages and cotton wool spots. En face OCTA montage (B) and FA (C) depict associated collateral vessel formation (red arrows), which are blocked by the dense hemorrhage on fundus photos. Yellow arrows indicate areas obscured by the extensive retinal hemorrhage on fundus photo, OCTA and FA.

3.1. Role of FA in Retinal Vein Occlusion

FA is commonly used to assess the perfusion status in RVO as non-perfusion is a strong predictor for the development of neovascularization [51]. In most RVO cases, FA demonstrates normal retinal arterial and choroidal filling, delayed retinal venous filling, variable staining of retina veins, and possible areas of capillary non-perfusion and retinal vascular leakage that results in retinal edema. In the presence of significant vision loss, FA can help assess the visual prognosis by differentiating between macular edema, which may improve with treatment or macular ischemia where the visual prognosis is guarded [52]. In the acute stages of RVO, the role of FA in assessing peripheral non-perfusion is limited due to blockage from dense intra-retinal hemorrhages (Figure 4C—yellow arrows) [47].

3.2. Role of OCTA in Retinal Vein Occlusion

Kashani et al. reported on OCTA findings in 25 eyes with RVO and found that OCTA is capable of visualizing peripheral pathology associated with vein occlusions, such as tortuous venous segments, areas of non-perfusion, retinal atrophy, collateral or shunt vessels, neovascularization as well as macula changes such as intraretinal edema and enlargement of the FAZ (Figures 4–6). These OCTA findings have been shown to be consistent with clinical, anatomic, and FA findings [53–55].

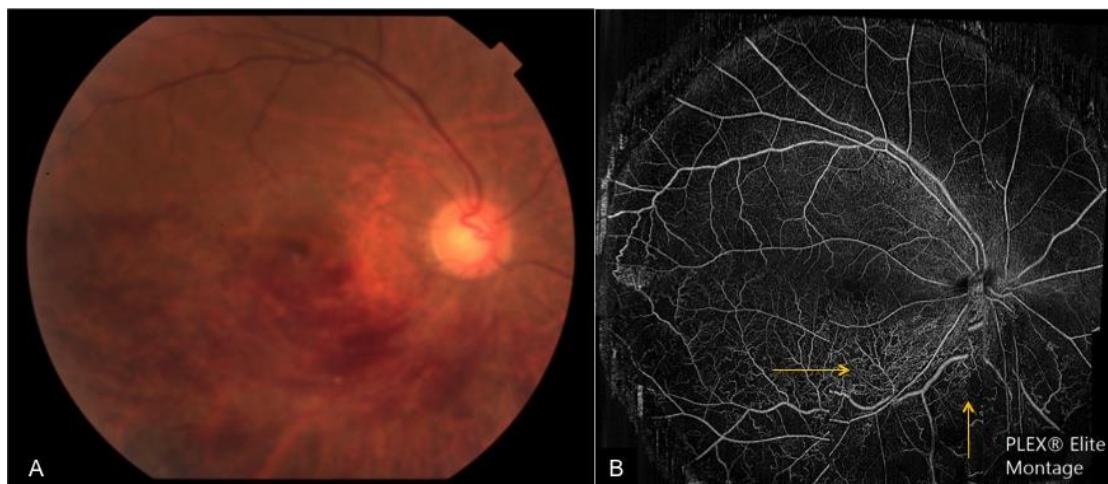


Figure 5. A case of chronic inferior branch retinal vein occlusion. (A): Color fundus photograph depicting inferior flame-shaped hemorrhages obscuring the view of the retina; (B): enface OCTA montage depicting inferior tortuous venous segments and associated collateral vessels (yellow arrows), which are obscured by hemorrhage on the corresponding fundus photograph.

Seknazi et al. used a commercially available automated angio-analytics software to quantify vascular density in the SCP, DCP, and FAZ, and showed that areas of capillary dropout correlated well with areas of peripheral non-perfusion on FA. They also found that decreased vascular density in the DCP correlated with poorer visual acuity [55]. Worsening severity of RVO has also been shown to be associated with a lower vascular skeletal density on OCTA. However, correlation between skeletal density and visual acuity was not explored in this study [56]. Studies of OCTA in vein occlusions have revealed that microvascular occlusion is more pronounced in the deep venous plexus compared with the superficial venous plexus in RVO [57]. Adhi and colleagues studied 23 patients with RVO and found a decrease in vascular perfusion at the deep plexus in all eyes with a RVO without cystoid macular edema [58]. Recent advances in OCTA technology have enabled wide-field OCTA imaging through an extended field imaging technique or swept source OCTA systems that can capture and montage 12 mm × 12 mm OCTA images and have been used to demonstrate that vascular length on OCTA correlates with areas of non-perfusion on FA [54,59]. Freund et al. recently published a paper studying the growth of collateral vessels associated with RVO and found that collateral vessels are

predominantly located within and course through the DCP. This has helped to further understanding of re-perfusion in chronic stages of RVOs [60].

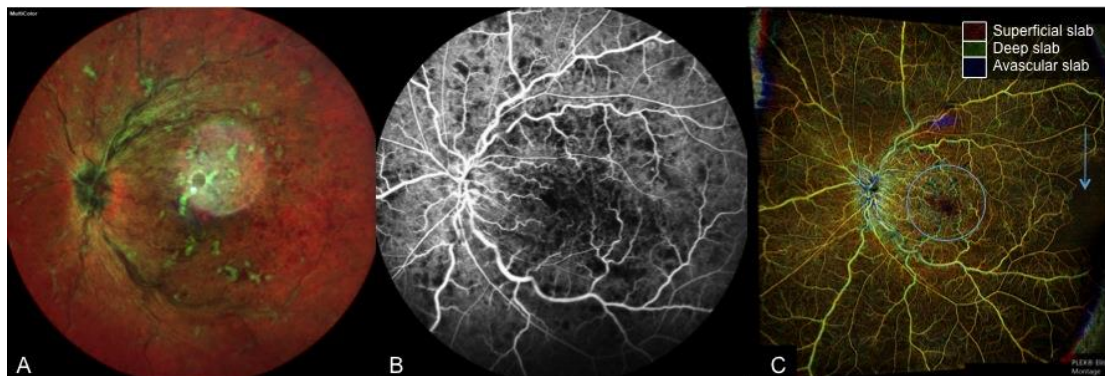


Figure 6. A case of central retinal vein occlusion. (A): Multi-color fundus photograph depicting tortuous venous segments, dot, blot, and flame hemorrhages and cotton wool spots. (B): FA depicting dilated and tortuous retina veins with patchy areas blocked by retina hemorrhage. (C): color-coded depth-resolved en face OCTA, which is a fusion image of the superficial (red), deep (green), and avascular (blue) en face OCTA slabs. An enlarged fovea avascular zone (blue circle) and temporal loss of flow (blue arrow), which is not depicted on FA, is seen on OCTA.

OCTA has also been an effective modality for assessing the macular complications of RVO. Nobre et al. evaluated 81 eyes with a history of RVO and found good agreement between FA and OCTA scans centered on the macula for capillary non-perfusion and capillary changes such as dilation, pruning, and telangiectasia (Figure 6—blue circle). The group also found good agreement for grading the FAZ for the 3 mm × 3 mm OCTA scan [61]. Hence, when used in conjunction with cross-sectional and en face structural OCT, OCTA may be able to provide enough information for the diagnosis of macular edema and ischemia, monitor response to therapy and assess visual prognosis, thus reducing the need for FA [14,53]. A limitation of OCTA, which is also seen in FA, is that microvascular alterations can be obscured by extensive intraretinal hemorrhages in the acute stage (Figure 4A—yellow arrows, Figure 5A). In addition, in cases where the visual acuity is impaired due to macular ischemia or severe macular edema, fixation may be challenging resulting in poor quality OCTA scan with movement or blink artefacts.

4. Retinal Artery Occlusion

Central retinal artery occlusion (CRAO) is an ophthalmic emergency and the majority of cases are caused by atherosclerosis-related thrombosis or occlusion of the retinal arteries by emboli [16]. The incidence of CRAO is linked to older age, hypertension, hyperlipidemia, carotid artery disease, diabetes, and smoking [62]. CRAO often foreshadows cerebrovascular or cardiovascular events [16,62].

In the acute stage, the compromised capillary blood flow leads to axoplasmic stasis, intracellular edema, and ischemic necrosis of the inner retinal layers [63]. Examination in CRAO reveals retinal edema and pallor over the affected area, a cherry red spot, cattle trucking, arterial attenuation, and optic disc edema [16]. After the acute stage, resolution of retinal edema is observed with the development of residual inner retinal atrophy and attenuation of vessels [63]. Clinical findings in chronic CRAOs are optic atrophy, retinal arterial attenuation, cilioretinal collaterals, and macular retinal pigment epithelium changes [62–64]. A long-term complication of CRAO is the risk of neovascularization and in some cases subsequent secondary glaucoma [62,65]. However, the etiology is controversial as some have found no cause-and-effect relationship between CRAO and neovascular glaucoma [66]. In general, the visual prognosis in CRAO is poor with 61% of patients having a final visual acuity of 20/400 or worse [16].

4.1. Current Imaging Techniques for Central Retinal Artery Occlusion

Multimodal imaging can be used to describe characteristics of acute retinal ischemia. Acute retinal ischemia on SD-OCT appears as thickening of the inner retina layers and loss of structure down to the outer plexiform layer. On fundus autofluorescence photos (FAF), darker areas correspond to thickened ischemic tissue with speckled regions occurring at the posterior pole in general hypoperfusion. Peri-arterial regions show normal FAF signal while peri-venous regions show decreased FAF signal intensity, which can create a 'frosted branch' appearance [67].

FA reveals important information regarding large vessel flow and is useful in demonstrating the delay in arterial filling and decreased capillary density corresponding to areas of occluded artery. Acutely, there are areas of hypofluorescence of the involved segment due to the blockage of background fluorescence by inner retinal swelling [63]. However, studies have shown that FA provides incomplete assessment of the SCP and even less information on the DCP. Therefore, FA is limited in studying microvascular histopathological processes [68].

4.2. Role of OCTA in Central Retinal Artery Occlusion

OCTA technology provides us with a means to assess the microvascular structures across all retinal layers and has a potential role in diagnosing, assessing the extent of macular ischemia, and monitoring disease progression in CRAO [14,64,69]. Currently, there are only a few studies on the role of OCTA in CRAO.

Feucht et al. found that areas of acute retinal ischemia appeared as areas of non-perfusion in the SCP, DCP, outer retina, and choriocapillaris layers. This was accompanied by a loss of capillary density, which was most marked in the SCP and DCP. Capillary flow was found to be below the limit of detection, but arteriole flow remained detectable. In contrast, well-perfused areas had larger retinal arteries and veins in the superficial plexus. They also showed that the choriocapillaris demonstrated reduced signal intensity in the area of occlusion that correlated to areas of inner retina edema and hyperreflectivity. Findings in the outer retina were confounded by the altered flow projections from the inner retina [67].

Hautz et al. reported on four cases of RAO in children using OCT and OCTA. In the acute stage, OCTA images showed ischemic changes in the SCP and DCP. OCTA images on follow-up revealed increasing areas of ischemia that appeared as a darker, smooth background, persistent narrowing of arteries, and loss of the capillary network (Figure 7) [70].

Bonini et al. conducted a case study of 7 patients with acute or chronic CRAO and BRAO. They found that OCTA showed decreased vascular perfusion in both the SCP and DCP that corresponded to areas of delayed perfusion on FA. In patients with acute and chronic CRAO, they found equal areas of decreased vascular perfusion in the SCP and DCP (Figure 7B,C). However, in a patient with chronic CRAO with cilioretinal sparing there was focal restoration of the deep capillary plexus perfusion in the macula region. 75% of their cases of acute and chronic BRAO showed focal restoration of the deep capillary plexus perfusion where the superficial capillary plexus perfusion is abnormal. Hence, with OCTA imaging, which allows the ability to differentiate between the superficial and deep vascular networks, it is now possible to image in subacute RAO cases, recanalization and reorganization of vascular interconnections that may contribute to partial restoration of the deep capillary plexus in areas where the superficial capillary plexus is still abnormal. A limitation of this study is that they did not segregate acute and chronic patients when analyzing OCTA findings. In addition, this study did not correlate re-perfusion with visual function [63].

OCTA is limited in retina ischemia as it only allows the evaluation of a snapshot of blood flow over time. Artefacts from the inner retina layers in acute ischemia also affect visibility of the outer retina [67]. The role of OCTA in chronic RAO is also limited due to difficulty with auto-segmenting layers of atrophic and thinned retina accurately [63]. In many cases, recanalization of the large vessels may occur and abnormal areas of flow may not be clearly evident in the presence of the thinned inner retina and OCTA images of cases with chronic RAO may even appear normal [71].

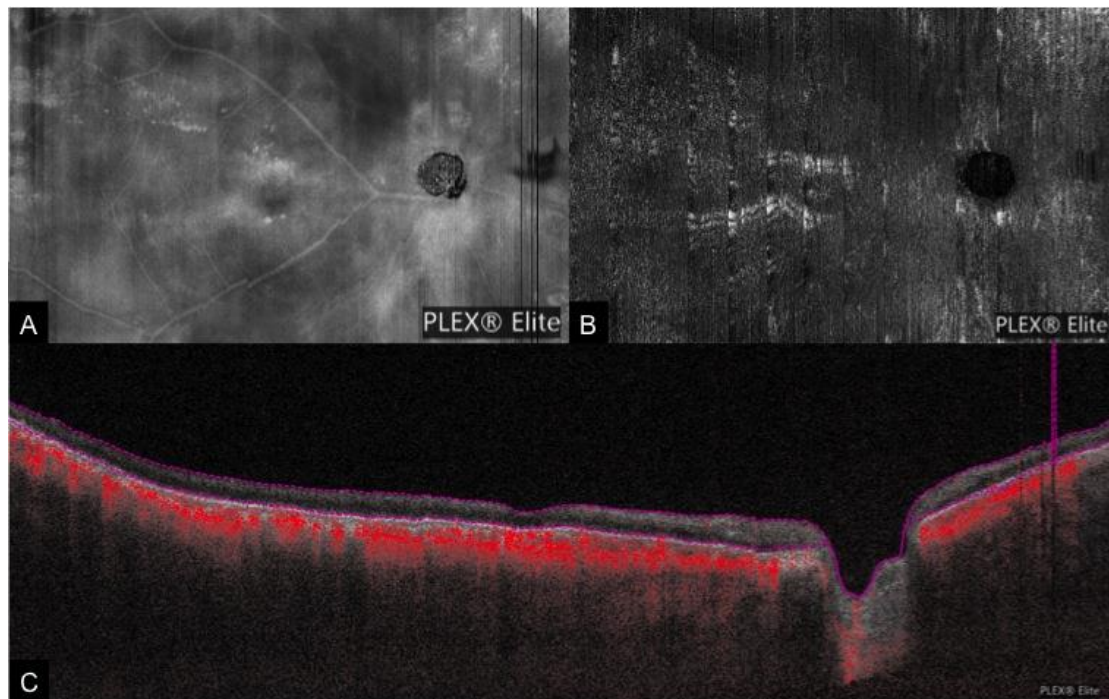


Figure 7. A case of right chronic central retinal artery occlusion. (A): Wide-field en face structural OCT demonstrating the presence of retinal vessels. However, the en face OCTA (B) shows no flow signal and the cross-sectional OCTA (C) shows that the retinal layers (bounded by red lines) are devoid of flow signal.

5. Ocular Ischemic Syndrome

Ocular ischemic syndrome (OIS) is the result of the chronic hypoperfusion of the eye due to atherosclerotic stenosis and occlusion of the common or internal carotid arteries. It is usually unilateral, presents in middle age, and commonly affects men. Carotid artery disease is associated with diabetes, hypertension, hyperlipidemia, and ischemic heart disease [72,73]. In OIS, there is decreased blood flow in retrobulbar vessels and even reversal of blood flow in the ophthalmic artery due to shunting of blood away from the eye to the low-resistance intracranial circuit [72]. Vascular complications in the anterior segment include iris rubeosis, neovascular glaucoma, and uveitis. Classically, in the posterior segment, mid-peripheral retinal dot-blot hemorrhages are seen. Other signs include narrowed retinal arteries, dilated veins, neovascularization of the disc or retina, cotton wool spots, vitreous hemorrhage, emboli, spontaneous arterial pulsations, and macular edema [73].

5.1. Current Imaging Techniques for Ocular Ischaemic Syndrome

FA is useful in establishing the diagnosis of OIS. OIS eyes frequently have prolonged retina arteriovenous transit time and often have patchy or delayed choroidal filling. Staining of retinal vessels occurs and is more pronounced for arteries in OIS, where conversely, in CRVO the staining of veins is more pronounced and in DR no vessel staining is usually seen. Vessel staining in OIS can also be associated with leakage. Occasionally, a well-demarcated leading edge of dye and macular edema can be observed. ICG is also useful for evaluating OIS and often shows a prolonged arm-to-choroid time prolonged intrachoroidal circulation time. Areas of chroidal hypoperfusion, filling defects, and slow filling of watershed zones of the choroid and choriocapillaris can also be observed [72].

A prominent middle limiting membrane sign on SD-OCT can be appreciated in patients with OIS. This segment is found between the outer plexiform layer and ganglion cell layer and is accentuated in peri-venous areas. It is likely that this region represents the location with the largest deficit of oxygen.

However, in CRAO, this sign is overshadowed by the increased reflectivity and thickness of the inner retinal layers [67].

5.2. Role of OCTA in Ocular Ischemic Syndrome

Presently, there are limited studies detailing the role of OCTA in OIS. OCTA has been shown to be comparable to dye-based angiography in imaging other retinal vascular diseases and ischemia of the optic nerve [74]. Similarly, in OIS, OCTA has a potential role in imaging areas of capillary hypoperfusion, retinal vascular abnormalities, intraretinal fluid, and neovascularization in both the anterior and posterior segment [67]. OCTA can also delineate areas of non-perfusion in the SCP, DCP, outer retina, and choriocapillary layers, and demonstrate the loss of capillary density in the SCP and DCP (Figure 8).

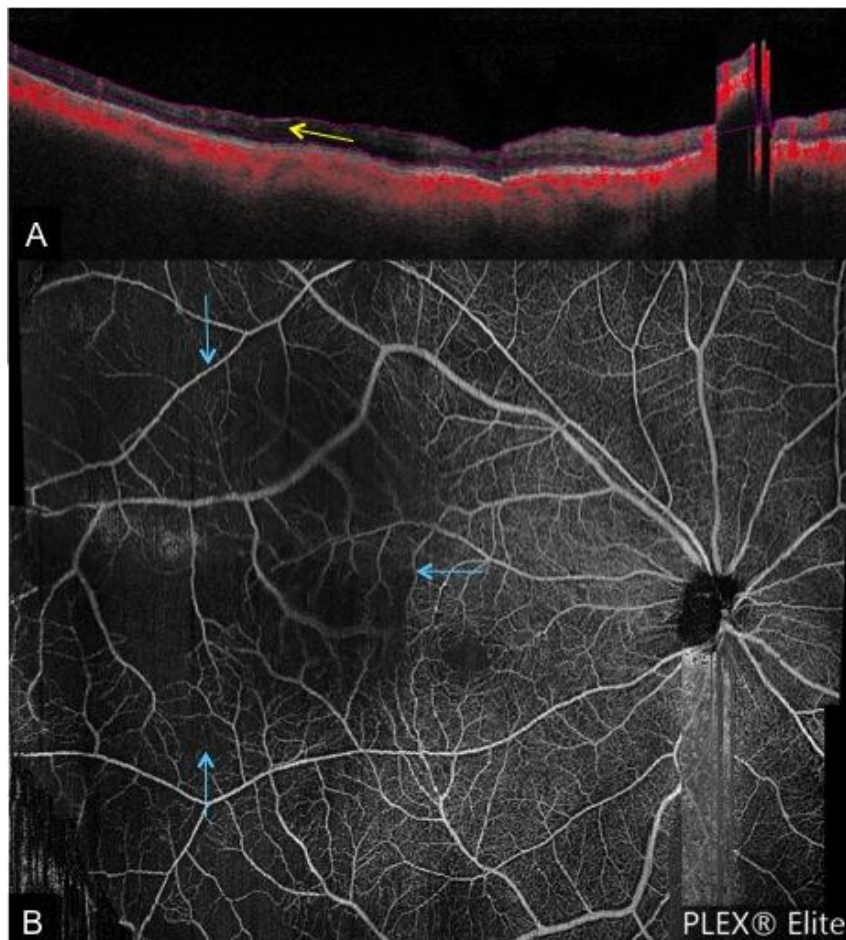


Figure 8. A case of ocular ischemic syndrome. (A): Cross-sectional OCTA showing temporal thinning of the retina layer in the posterior pole (indicated by the yellow arrow) along with a reduced flow signal. (B): Corresponding en face OCTA demonstrating reduced flow in the temporal region (blue arrows).

OCTA can also show the presence of collateral “shunting” vessels in OIS as demonstrated in the case study by Lupidi et al. [75]. While FA gives useful information on the presence and activity of neovascularization, OCTA is effective in identifying the origin of new vessels, anatomical and topographical relationships of neovascularization with different retinal structures and how they change after intravitreal and laser treatment [75]. It should be noted, however, that outer retina findings on OCTA may be affected by artefact if inner retina ischemia is present [67].

Saito et al. have recently used OCTA to compare changes in the superficial and deep FAZ and vessel density before and after carotid artery stenting in a patient with OIS. They found that enhanced

blood flow after stenting was accompanied by a reduction in the FAZ area and increased vessel density in the superficial and deep layers. One of their hypotheses is that capillary blood flow slows toward the periphery of the FAZ and may fall below the threshold necessary for OCTA detection in patients with OIS. Thus, once capillary flow velocity is improved after carotid stenting, the FAZ can seem to decrease in size on OCTA in OIS. This study also shows the potential to use OCTA to track changes in individual auto segmented retinal layers for patients in order to study the impact of disease and treatment on retina vasculature [76].

6. Iris Neovascularization

Neovascularization of the iris (NVI) and the angle can occur secondary to diabetes mellitus, but also from secondary causes such as ischemia of the anterior segment following retinal vein occlusion or even long-standing mild ocular ischemia. In severe stages of DR new vessels are not confined to the retina and can grow around the pupillary border and the root of iris and can penetrate the anterior surface of the iris in severe cases. These abnormal iris vessels or 'rubeosis' often leads to serious complications such as spontaneous hyphema and the often sight-threatening complication of neovascular glaucoma (NVG) [77]. Thus, it is useful to detect NVI at its early stage as prompt treatment may prevent the development of NVG.

However, NVI is often diagnosed late in the clinic, with careful slit-lamp examination and gonioscopy required to diagnose NVI (Figure 9A). At times, NVI are identified incidentally during FA and ICG. However, these invasive imaging modalities are not ideal for solely screening for iris neovascularization. Moreover, patients may require two visits if both iris and retina angiograms need to be taken as the iris is imaged with the iris undilated and the retina is imaged with the iris dilated. Therefore, FA and ICG are not commonly used to image anterior segment and iris vasculature [3,78].

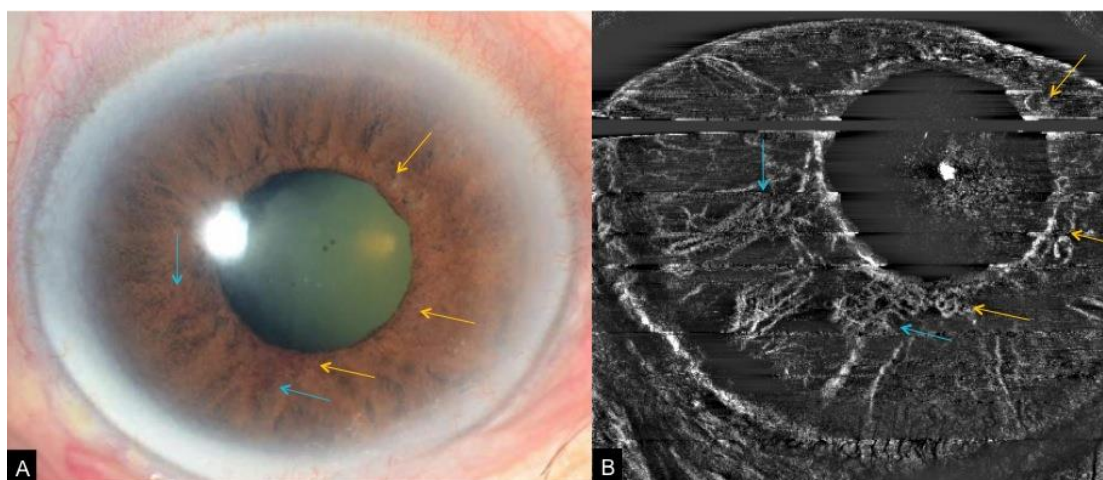


Figure 9. A case of iris neovascularization secondary to ocular ischemic syndrome. Slit lamp photograph (A) corresponding OCTA of the iris (B) showing fine new vessels at the pupillary border (yellow arrows) and slightly larger new vessels on the anterior surface of the iris (blue arrows).

6.1. OCTA for Iris Neovascularization

A potential alternative is the use of OCTA adapted for the anterior segment. [5] While current commercially available OCTA are designed to examine the posterior segment of the eye, an adapter lens can provide high-quality images of the anterior segment vasculature with good inter-observer agreement for qualitative measurements [1]. Roberts et al. showed neovascularization of the iris is characterized on OCTA by random orientation of vessels, significant tortuosity, and smaller caliber (Figure 9B). They demonstrated that OCTA is also effective in detecting subclinical NVI [6]. Roberts et al. proposed staging criteria for NVI using en face and cross-sectional OCTA based on the established staging system by Gartner and Henkind. Stage 1 is defined when fine, thin-walled irregular

vessels at the pupillary border and iris root are visualized, stage 2 is where these vessels enlarge and penetrate to the anterior iris surface and stroma, and stage 3 is where two sets of NVI merge and this NVI covers parts of the anterior surface of the iris, with or without the presence of peripheral anterior synechiae. They added a fourth stage for regressed NVI seen after treatment [6].

OCTA has a role in the evaluation of anterior segment vasculature in the setting of anti-angiogenic therapy, where regression of NVI can serve as markers of VEGF levels therefore guiding re-treatment decisions [4]. This may become a useful tool for clinical surveillance of proliferative and ischemic changes in DR [37]. However, OCTA of the anterior segment is still limited as it cannot visualize leakage and hence activity of new vessels [79].

6.2. Limitations of OCTA for Iris Neovascularization

Adapting OCTA for the anterior segment to detect iris neovascularization has a few limitations. Firstly, current OCTA systems are not optimized for the anterior segment [10,80]. The scanning protocols have to be altered and specialised anterior segment adaptive lenses have to be used [78,80]. The field of view is also limited compared to angiography techniques at present [78].

Secondly, anterior segment OCTA is incapable of registering scans and providing localization required for comparison of serial scans [1,81]. Additional image processing software is still to overcome this limitation.

Anterior segment OCTA is also prone to artefact. Motion artefacts are common in anterior scans due to saccadic eye movements. There is currently a lack of motion correction software and still an unmet need for specialised eye-tracking systems built specifically for the anterior segment [10,82]. Current OCTA software is also designed to image the posterior segment, which can result in non-parallel segmentation and artefacts when used for the anterior segment due to the curvature of the cornea [83]. Additionally, anterior OCTA is also prone to artefacts from hyper-reflective structures such as corneal fibrosis or scarring [80]. Vessels in the superficial layers can also create projection artefacts in the deeper layers, which can be misinterpreted by the software as abnormal or additional vessels [5]. Therefore, it is important to compare the scans with serial scans, corresponding structural OCT, and slit lamp photographs.

In OCTA, dense iris pigmentation affects visualization of deeper stromal vessels, as also seen in FA and ICG [5]. As NVI develops on the surface of the iris, distinction of NVI by OCTA is much easier in eyes with darker irises. Conversely, light irises require more careful evaluation of en face angiographic images to differentiate between physiological and pathological vessels. Out of these options, ICG still has better penetration through pigment as it is performed using near-infrared wavelengths [6].

Lastly, anterior segment OCTA is also unable to visualise deeper vessels in eyes with corneal opacities, dense iris pigmentation, or vessels in thick iris tumours [81]. The systems also have poorer detection of vessels with minimal flow since erythrocytes are slower in small calibre vessels and may be below the threshold of detection, which is dependent on the A-scan rate of the system [80]. OCTA is also unable to differentiate between arteries and veins [84]. As OCTA algorithms are optimized for the posterior segment, which has mainly transverse flow in vessels, anterior segment vessels with axial flow may also not be detected [85].

7. General Limitations of OCTA

While OCTA may seem comparable to FFA and ICG in studies, there are still many limitations that need to be considered, especially in imaging of the retina and posterior segment. Firstly, current commercial OCTA platforms have a limited field of view. At present, en-face OCTA scanning area ranges from 2 mm × 2 mm to 12 mm × 12 mm. Due to limitations in scanning speed and image resolution, increasing the field of view worsens the degree of resolution and increases the time taken to capture the image, thus also potentially increasing the risk of more artefacts. Recent studies have described an extended field technique, which uses optical aid attachments on current OCTA machines to increase the field of view [59,86]. Creating a montage of multiple separate OCTA images to obtain

a high resolution wide-field image is also possible and is an automated function available on some machines. However taking multiple OCTA images of different retina areas is time consuming and will require good fixation by the patient for good quality images [3,4,78].

As OCTA relies on change between consecutive B-scans, the slowest detectable flow is limited by the time between consecutive scans. Therefore, areas of slow blood flow such as in MAs, thrombi and fibrotic choroidal neovascularization can be missed [4]. Studies have also demonstrated that fewer MAs are visualized on OCTA compared to FA [4,24]. In addition, as flow information is only acquired at a fixed point in time, leakage is not appreciable on OCTA [3].

OCTA also relies on auto segmentation technology to delineate different retina layers. En face segmentation defects are common in edema or retina thinning where the normal retina anatomy has been disrupted. In addition, layer segmentation methods and definitions are not standardized, which may create discrepancies between studies. Inaccurate automated segmentation may have to be adjusted manually to better capture accurately the various venous plexi [4,7]. Thus, it is important to look at OCTA images and structural OCT images in tandem in order to overcome this.

OCTA may also be prone to artefact. The validity and reproducibility automated quantification of various parameters measured in the SCP and DCP are dependent on not only accurate segmentation but also the lack of projection artefact. Projection artefacts occur when more superficial flow signals are projected onto deeper retina layers [87]. One recent study showed that projection-resolved OCTA parameters significantly improved the vascular density analysis of the DCP [33]. Other artefacts include shadow artefacts from larger retinal vessels and artefacts created by fine movement from pigment epithelial defects and fine tissue [3]. Like other optical imaging systems, OCTA images can also be confounded by speckle artefact. Development of speckle noise reduction software may allow for clearer image acquisition and segmentation [88–90]. In addition, the OCTA system also requires good fixation from the patient and is sensitive to motion and blink artefact [3].

Multiple vendors currently produce OCTA technology so variations in hardware and software algorithms need to be taken into account [6,10,78,80]. With the increasing availability of automated quantitative parameters, it is mindful to note that the images and quantification are not comparable between different OCTA systems [91]. Lastly, although a trained technician can easily obtain OCTA images, there is still a significant learning curve to overcome when it comes to image interpretation [3].

8. Wider Applications and Conclusions

In this rapidly advancing field, it is likely that many of these limitations will be overcome in the coming years. With the development of better eye-tracking technology, higher imaging speeds, newer montage software, and improved image processing and artefact reduction, more wide-field, high-definition OCTA imaging will become available.

OCTA is a very promising technology that enables clinicians to effortlessly image both anterior and posterior segment pathology. There are numerous other uses for OCTA in glaucoma, uveitis, cornea, and optic nerve pathology, along with extra-ocular diseases such as coronary artery disease, which are not mentioned in this review.

Today, systemic vascular diseases are on the rise worldwide and an increasing number of people are suffering from sight-threatening complications due to diabetes, vein occlusions, and ischemic ocular conditions. OCTA provides us with an accessible way to study anterior and posterior segment microvasculature in depth and opens more possibilities for screening, diagnosing and monitoring of ocular vascular diseases.

Author Contributions: Writing—original draft preparation, C.L.W.; writing—review and editing, M.A., A.C.S.T.; supervision, A.C.S.T.

Funding: This research received no external funding.

Conflicts of Interest: The authors declare no conflict of interest.

References

1. Ang, M.; Baskaran, M.; Werkmeister, R.M.; Chua, J.; Schmidl, D.; Aranha dos Santos, V.; Garhöfer, G.; Mehta, J.S.; Schmetterer, L. Anterior segment optical coherence tomography. *Prog. Retin. Eye Res.* **2018**, *66*, 132–156. [CrossRef] [PubMed]
2. Chua, J.; Tan, B.; Ang, M.; Nongpiur, M.E.; Tan, A.C.; Najjar, R.P.; Milea, D.; Schmetterer, L. Future clinical applicability of optical coherence tomography angiography. *Clin. Exp. Optom.* **2019**, *102*, 260–269. [CrossRef] [PubMed]
3. de Carlo, T.E.; Romano, A.; Waheed, N.K.; Duker, J.S. A review of optical coherence tomography angiography (OCTA). *Int. J. Retina Vitre.* **2015**, *1*, 5. [CrossRef] [PubMed]
4. Spaide, R.F.; Fujimoto, J.G.; Waheed, N.K.; Sadda, S.R.; Staurengghi, G. Optical coherence tomography angiography. *Prog. Retin. Eye Res.* **2018**, *64*, 1–55. [CrossRef] [PubMed]
5. Lee, W.D.; Devarajan, K.; Chua, J.; Schmetterer, L.; Mehta, J.S.; Ang, M. Optical coherence tomography angiography for the anterior segment. *Eye Vis.* **2019**, *6*, 4. [CrossRef] [PubMed]
6. Roberts, P.K.; Goldstein, D.A.; Fawzi, A.A. Anterior Segment Optical Coherence Tomography Angiography for Identification of Iris Vasculature and Staging of Iris Neovascularization: A Pilot Study. *Curr. Eye Res.* **2017**, *42*, 1136–1142. [CrossRef] [PubMed]
7. Kashani, A.H.; Chen, C.-L.; Gahm, J.K.; Zheng, F.; Richter, G.M.; Rosenfeld, P.J.; Shi, Y.; Wang, R.K. Optical Coherence Tomography Angiography: A Comprehensive Review of Current Methods and Clinical Applications. *Prog. Retin. Eye Res.* **2017**, *60*, 66–100. [CrossRef]
8. Chen, C.-L.; Wang, R.K. Optical coherence tomography based angiography. *Biomed. Opt. Express* **2017**, *8*, 1056–1082. [CrossRef]
9. Hong, Y.-J.; Miura, M.; Makita, S.; Ju, M.J.; Lee, B.H.; Iwasaki, T.; Yasuno, Y. Noninvasive Investigation of Deep Vascular Pathologies of Exudative Macular Diseases by High-Penetration Optical Coherence Angiography. *Investig. Ophthalmol. Vis. Sci.* **2013**, *54*, 3621–3631. [CrossRef]
10. Ang, M.; Tan, A.C.S.; Cheung, C.M.G.; Keane, P.A.; Dolz-Marco, R.; Sng, C.C.A.; Schmetterer, L. Optical coherence tomography angiography: A review of current and future clinical applications. *Graefes Arch. Clin. Exp. Ophthalmol.* **2018**, *256*, 237–245. [CrossRef]
11. Kirwan, R.P.; Zheng, Y.; Tey, A.; Anijeet, D.; Sueke, H.; Kaye, S.B. Quantifying changes in corneal neovascularization using fluorescein and indocyanine green angiography. *Am. J. Ophthalmol.* **2012**, *154*, 850–858.e2. [CrossRef] [PubMed]
12. Spaide, R.F.; Klancnik, J.M.; Cooney, M.J. Retinal Vascular Layers Imaged by Fluorescein Angiography and Optical Coherence Tomography Angiography. *JAMA Ophthalmol.* **2015**, *133*, 45–50. [CrossRef] [PubMed]
13. NCDs|Noncommunicable Diseases and Their Risk Factors. Available online: <http://www.who.int/ncds/en/> (accessed on 8 April 2019).
14. Sambhav, K.; Grover, S.; Chalam, K.V. The application of optical coherence tomography angiography in retinal diseases. *Surv. Ophthalmol.* **2017**, *62*, 838–866. [CrossRef] [PubMed]
15. Chalam, K.V.; Sambhav, K. Optical Coherence Tomography Angiography in Retinal Diseases. *J. Ophthalmic Vis. Res.* **2016**, *11*, 84–92. [CrossRef] [PubMed]
16. Chen, C.S.; Lee, A.W. Management of acute central retinal artery occlusion. *Nat. Rev. Neurol.* **2008**, *4*, 376–383. [CrossRef] [PubMed]
17. WHO|Priority Eye Diseases. Available online: <http://www.who.int/blindness/causes/priority/en/index1.html> (accessed on 13 March 2015).
18. Ciulla, T.A.; Amador, A.G.; Zinman, B. Diabetic Retinopathy and Diabetic Macular Edema Pathophysiology, screening, and novel therapies. *Diabetes Care* **2003**, *26*, 2653–2664. [CrossRef] [PubMed]
19. Grading diabetic retinopathy from stereoscopic color fundus photographs—An extension of the modified Airlie House classification. ETDRS report number 10. Early Treatment Diabetic Retinopathy Study Research Group. *Ophthalmology* **1991**, *98*, 786–806. [CrossRef]
20. Lee, R.; Wong, T.Y.; Sabanayagam, C. Epidemiology of diabetic retinopathy, diabetic macular edema and related vision loss. *Eye Vis.* **2015**, *2*, 17. [CrossRef]
21. Gupta, N.; Mansoor, S.; Sharma, A.; Sapkal, A.; Sheth, J.; Falatoonzadeh, P.; Kuppermann, B.; Kenney, M. Diabetic Retinopathy and VEGF. *Open Ophthalmol. J.* **2013**, *7*, 4–10. [CrossRef]

22. Wu, L.; Fernandez-Loaiza, P.; Sauma, J.; Hernandez-Bogantes, E.; Masis, M. Classification of diabetic retinopathy and diabetic macular edema. *World J. Diabetes* **2013**, *4*, 290–294. [[CrossRef](#)]
23. Classification of Diabetic Retinopathy from Fluorescein Angiograms: ETDRS Report Number 11. *Ophthalmology* **1991**, *98*, 807–822. [[CrossRef](#)]
24. Matsunaga, D.; Yi, J.; Olmos, L.C.; Legarreta, J.; Legarreta, A.D.; Gregori, G.; Sharma, U.; Rosenfeld, P.J.; Puliafito, C.A.; Kashani, A.H. OCT Angiography (OCTA) of Diabetic Retinopathy. *Investig. Ophthalmol. Vis. Sci.* **2015**, *56*, 3335.
25. Lee, J.; Rosen, R. Optical Coherence Tomography Angiography in Diabetes. *Curr. Diabetes Rep.* **2016**, *16*, 123. [[CrossRef](#)] [[PubMed](#)]
26. Ishibazawa, A.; Nagaoka, T.; Yokota, H.; Takahashi, A.; Omae, T.; Song, Y.-S.; Takahashi, T.; Yoshida, A. Characteristics of Retinal Neovascularization in Proliferative Diabetic Retinopathy Imaged by Optical Coherence Tomography Angiography. *Investig. Ophthalmol. Vis. Sci.* **2016**, *57*, 6247–6255. [[CrossRef](#)]
27. Li, Z.; Alzogool, M.; Xiao, J.; Zhang, S.; Zeng, P.; Lan, Y. Optical coherence tomography angiography findings of neurovascular changes in type 2 diabetes mellitus patients without clinical diabetic retinopathy. *Acta Diabetol.* **2018**, *55*, 1075–1082. [[CrossRef](#)] [[PubMed](#)]
28. de Carlo, T.E.; Chin, A.T.; Bonini Filho, M.A.; Adhi, M.; Branchini, L.; Salz, D.A.; Bauman, C.R.; Crawford, C.; Reichel, E.; Witkin, A.J.; et al. Detection of Microvascular changes in eyes of patients with diabetes but not clinical diabetic retinopathy using optical coherence tomography angiography. *Retina (Phila. Pa.)* **2015**, *35*, 2364–2370. [[CrossRef](#)] [[PubMed](#)]
29. Salz, D.A.; de Carlo, T.; Adhi, M.; Moulton, E.; Choi, W.J.; Bauman, C.R.; Witkin, A.J.; Duker, J.S.; Fujimoto, J.G.; Waheed, N.K. Prototype Ultra-High Speed Swept Source Optical Coherence Tomography Angiography compared with Intravenous Fluorescein Angiography in Diabetic Retinopathy. *Investig. Ophthalmol. Vis. Sci.* **2015**, *56*, 3341.
30. Matsunaga, D.R.; Yi, J.J.; De Koo, L.O.; Ameri, H.; Puliafito, C.A.; Kashani, A.H. Optical Coherence Tomography Angiography of Diabetic Retinopathy in Human Subjects. *Ophthalmic Surg. Lasers Imaging Retina* **2015**, *46*, 796–805. [[CrossRef](#)]
31. Scarinci, F.; Nesper, P.L.; Fawzi, A.A. Deep Retinal Capillary Nonperfusion Is Associated With Photoreceptor Disruption in Diabetic Macular Ischemia. *Am. J. Ophthalmol.* **2016**, *168*, 129–138. [[CrossRef](#)]
32. Rodrigues, T.M.; Marques, J.P.; Soares, M.; Simão, S.; Melo, P.; Martins, A.; Figueira, J.; Murta, J.N.; Silva, R. Macular OCT-angiography parameters to predict the clinical stage of nonproliferative diabetic retinopathy: An exploratory analysis. *Eye* **2019**, *1*. [[CrossRef](#)]
33. Binotti, W.W.; Romano, A.C. Projection-Resolved Optical Coherence Tomography Angiography Parameters to Determine Severity in Diabetic Retinopathy. *Investig. Ophthalmol. Vis. Sci.* **2019**, *60*, 1321–1327. [[CrossRef](#)] [[PubMed](#)]
34. Ashraf, M.; Nesper, P.L.; Jampol, L.M.; Yu, F.; Fawzi, A.A. Statistical Model of Optical Coherence Tomography Angiography Parameters That Correlate with Severity of Diabetic Retinopathy. *Investig. Ophthalmol. Vis. Sci.* **2018**, *59*, 4292–4298. [[CrossRef](#)] [[PubMed](#)]
35. Onishi, A.C.; Nesper, P.L.; Roberts, P.K.; Moharram, G.A.; Chai, H.; Liu, L.; Jampol, L.M.; Fawzi, A.A. Importance of Considering the Middle Capillary Plexus on OCT Angiography in Diabetic Retinopathy. *Investig. Ophthalmol. Vis. Sci.* **2018**, *59*, 2167–2176. [[CrossRef](#)] [[PubMed](#)]
36. Elbendary, A.M.; Abouelkheir, H.Y. Bimodal imaging of proliferative diabetic retinopathy vascular features using swept source optical coherence tomography angiography. *Int. J. Ophthalmol.* **2018**, *11*, 1528–1533. [[PubMed](#)]
37. Hwang, T.S.; Jia, Y.; Gao, S.S.; Bailey, S.T.; Lauer, A.K.; Flaxel, C.J.; Wilson, D.J.; Huang, D. optical coherence tomography angiography features of diabetic retinopathy. *Retina (Phila. Pa.)* **2015**, *35*, 2371–2376. [[CrossRef](#)] [[PubMed](#)]
38. Tan, A.C.S.; Tan, G.S.; Denniston, A.K.; Keane, P.A.; Ang, M.; Milea, D.; Chakravarthy, U.; Cheung, C.M.G. An overview of the clinical applications of optical coherence tomography angiography. *Eye (Lond. Engl.)* **2018**, *32*, 262–286. [[CrossRef](#)] [[PubMed](#)]
39. Khadamy, J.; Abri Aghdam, K.; Falavarjani, K.G. An Update on Optical Coherence Tomography Angiography in Diabetic Retinopathy. *J. Ophthalmic Vis. Res.* **2018**, *13*, 487–497.

40. Agemy, S.A.; Sripsema, N.K.; Shah, C.M.; Chui, T.; Garcia, P.M.; Lee, J.G.; Gentile, R.C.; Hsiao, Y.-S.; Zhou, Q.; Ko, T.; et al. retinal vascular perfusion density mapping using optical coherence tomography angiography in normals and diabetic retinopathy patients. *Retina (Phila. Pa.)* **2015**, *35*, 2353–2363. [[CrossRef](#)]
41. Yasukura, S.; Murakami, T.; Suzuma, K.; Yoshitake, T.; Nakanishi, H.; Fujimoto, M.; Oishi, M.; Tsujikawa, A. Diabetic Nonperfused Areas in Macular and Extramacular Regions on Wide-Field Optical Coherence Tomography Angiography. *Investig. Ophthalmol. Vis. Sci.* **2018**, *59*, 5893–5903. [[CrossRef](#)]
42. Hasegawa, N.; Nozaki, M.; Takase, N.; Yoshida, M.; Ogura, Y. New Insights into Microaneurysms in the Deep Capillary Plexus Detected by Optical Coherence Tomography Angiography in Diabetic Macular Edema. *Investig. Ophthalmol. Vis. Sci.* **2016**, *57*, OCT348–OCT355. [[CrossRef](#)]
43. Mané, V.; Dupas, B.; Gaudric, A.; Bonnin, S.; Pedinielli, A.; Bousquet, E.; Erginay, A.; Tadayoni, R.; Couturier, A. Correlation between cystoid spaces in chronic diabetic macular edema and capillary nonperfusion detected by optical coherence tomography angiography. *Retina* **2016**, *36*, S102–S110. [[CrossRef](#)] [[PubMed](#)]
44. Moein, H.-R.; Novais, E.A.; Rebhun, C.B.; Cole, E.D.; Louzada, R.N.; Witkin, A.J.; Baumal, C.R.; Duker, J.S.; Waheed, N.K. Optical coherence tomography angiography to detect macular capillary ischemia in patients with inner retinal changes after resolved diabetic macular edema. *Retina (Phila. Pa.)* **2018**, *38*, 2277–2284. [[CrossRef](#)] [[PubMed](#)]
45. Karia, N. Retinal vein occlusion: Pathophysiology and treatment options. *Clin. Ophthalmol. (Auckl. N.Z.)* **2010**, *4*, 809–816. [[CrossRef](#)] [[PubMed](#)]
46. Rehak, M.; Wiedemann, P. Retinal vein thrombosis: Pathogenesis and management. *J. Thromb. Haemost.* **2010**, *8*, 1886–1894. [[CrossRef](#)] [[PubMed](#)]
47. Ehlers, J.P.; Fekrat, S. Retinal Vein Occlusion: Beyond the Acute Event. *Surv. Ophthalmol.* **2011**, *56*, 281–299. [[CrossRef](#)] [[PubMed](#)]
48. Clarkson, J.G. Central Vein Occlusion Study: Photographic protocol and early natural history. *Trans. Am. Ophthalmol. Soc.* **1994**, *92*, 203–215. [[PubMed](#)]
49. Kim, K.S.; Chang, H.R.; Song, S. Ischaemic change after intravitreal bevacizumab (Avastin®) injection for macular oedema secondary to non-ischaemic central retinal vein occlusion. *Acta Ophthalmol. (Copenh.)* **2008**, *86*, 925–927. [[CrossRef](#)] [[PubMed](#)]
50. Simó, R.; Hernández, C. Intravitreal anti-VEGF for diabetic retinopathy: Hopes and fears for a new therapeutic strategy. *Diabetologia* **2008**, *51*, 1574–1580. [[CrossRef](#)] [[PubMed](#)]
51. Natural history and clinical management of central retinal vein occlusion. The Central Vein Occlusion Study Group. *Arch. Ophthalmol. (Chic. Ill 1960)* **1997**, *115*, 486–491.
52. Ghashut, R.; Muraoka, Y.; Ooto, S.; Iida, Y.; Miwa, Y.; Suzuma, K.; Murakami, T.; Kadomoto, S.; Tsujikawa, A.; Yoshimura, N. Evaluation of macular ischemia in eyes with central retinal vein occlusion: An Optical Coherence Tomography Angiography Study. *Retina* **2018**, *38*, 1571–1580. [[CrossRef](#)] [[PubMed](#)]
53. Kashani, A.H.; Lee, S.Y.; Moshfeghi, A.; Durbin, M.K.; Puliafito, C.A. Optical coherence tomography angiography of retinal venous occlusion. *Retina* **2015**, *35*, 2323–2331. [[CrossRef](#)] [[PubMed](#)]
54. Shiraki, A.; Sakimoto, S.; Tsuboi, K.; Wakabayashi, T.; Hara, C.; Fukushima, Y.; Sayanagi, K.; Nishida, K.; Sakaguchi, H.; Nishida, K. Evaluation of retinal nonperfusion in branch retinal vein occlusion using wide-field optical coherence tomography angiography. *Acta Ophthalmol. (Copenh.)* **2019**. [[CrossRef](#)] [[PubMed](#)]
55. Seknazi, D.; Coscas, F.; Sellam, A.; Rouimi, F.; Coscas, G.; Souied, E.H.; Glacet-Bernard, A. OPTICAL COHERENCE TOMOGRAPHY ANGIOGRAPHY IN RETINAL VEIN OCCLUSION: Correlations Between Macular Vascular Density, Visual Acuity, and Peripheral Nonperfusion Area on Fluorescein Angiography. *Retina (Phila. Pa.)* **2018**, *38*, 1562–1570. [[CrossRef](#)] [[PubMed](#)]
56. Koullisis, N.; Kim, A.Y.; Chu, Z.; Shahidzadeh, A.; Burkemper, B.; de Koo, L.C.O.; Moshfeghi, A.A.; Ameri, H.; Puliafito, C.A.; Isozaki, V.L.; et al. Quantitative microvascular analysis of retinal venous occlusions by spectral domain optical coherence tomography angiography. *PLoS ONE* **2017**, *12*, e0176404. [[CrossRef](#)] [[PubMed](#)]
57. Coscas, F.; Glacet-Bernard, A.; Miere, A.; Caillaux, V.; Uzzan, J.; Lupidi, M.; Coscas, G.; Souied, E.H. Optical Coherence Tomography Angiography in Retinal Vein Occlusion: Evaluation of Superficial and Deep Capillary Plexa. *Am. J. Ophthalmol.* **2016**, *161*, 160–171.e2. [[CrossRef](#)] [[PubMed](#)]

58. Adhi, M.; Filho, M.A.B.; Louzada, R.N.; Kuehlewein, L.; de Carlo, T.E.; Baumal, C.R.; Witkin, A.J.; Satta, S.R.; Sarraf, D.; Reichel, E.; et al. Retinal Capillary Network and Foveal Avascular Zone in Eyes with Vein Occlusion and Fellow Eyes Analyzed with Optical Coherence Tomography Angiography. *Investig. Ophthalmol. Vis. Sci.* **2016**, *57*, OCT486–OCT494. [[CrossRef](#)] [[PubMed](#)]
59. Kimura, M.; Nozaki, M.; Yoshida, M.; Ogura, Y. Wide-field optical coherence tomography angiography using extended field imaging technique to evaluate the nonperfusion area in retinal vein occlusion. *Clin. Ophthalmol. (Auckl. N.Z.)* **2016**, *10*, 1291–1295. [[CrossRef](#)] [[PubMed](#)]
60. Freund, K.B.; Sarraf, D.; Leong, B.C.S.; Garrity, S.T.; Vupparaboina, K.K.; Dansingani, K.K. Association of Optical Coherence Tomography Angiography of Collaterals in Retinal Vein Occlusion with Major Venous Outflow Through the Deep Vascular Complex. *JAMA Ophthalmol.* **2018**, *136*, 1262–1270. [[CrossRef](#)]
61. Nobre Cardoso, J.; Keane, P.A.; Sim, D.A.; Bradley, P.; Agrawal, R.; Addison, P.K.; Egan, C.; Tufail, A. Systematic Evaluation of Optical Coherence Tomography Angiography in Retinal Vein Occlusion. *Am. J. Ophthalmol.* **2016**, *163*, 93–107.e6. [[CrossRef](#)]
62. Varma, D.D.; Cugati, S.; Lee, A.W.; Chen, C.S. A review of central retinal artery occlusion: Clinical presentation and management. *Eye* **2013**, *27*, 688–697. [[CrossRef](#)]
63. Bonini Filho, M.A.; Adhi, M.; de Carlo, T.E.; Ferrara, D.; Baumal, C.R.; Witkin, A.J.; Reichel, E.; Kuehlewein, L.; Satta, S.R.; Sarraf, D.; et al. Optical coherence tomography angiography in retinal artery occlusion. *Retina* **2015**, *35*, 2339–2346. [[CrossRef](#)] [[PubMed](#)]
64. Lee, A.Y.; Zhang, Q.; Baughman, D.M.; Mudumbai, R.; Wang, R.K.; Lee, C.S. Evaluation of bilateral central retinal artery occlusions with optical coherence tomography-based microangiography: A case report. *J. Med. Case Rep.* **2016**, *10*. [[CrossRef](#)] [[PubMed](#)]
65. Rudkin, A.K.; Lee, A.W.; Chen, C.S. Ocular neovascularization following central retinal artery occlusion: Prevalence and timing of onset. *Eur. J. Ophthalmol.* **2010**, *20*, 1042–1046. [[CrossRef](#)] [[PubMed](#)]
66. Hayreh, S.S.; Podhajsky, P.A.; Zimmerman, M.B. Retinal artery occlusion: Associated systemic and ophthalmic abnormalities. *Ophthalmology* **2009**, *116*, 1928–1936. [[CrossRef](#)] [[PubMed](#)]
67. Feucht, N.; Zapp, D.; Reznicek, L.; Lohmann, C.P.; Maier, M.; Mayer, C.S. Multimodal imaging in acute retinal ischemia: Spectral domain OCT, OCT-angiography and fundus autofluorescence. *Int. J. Ophthalmol.* **2018**, *11*, 1521–1527.
68. Mendis, K.R.; Balaratnasingam, C.; Yu, P.; Barry, C.J.; McAllister, I.L.; Cringle, S.J.; Yu, D.-Y. Correlation of histologic and clinical images to determine the diagnostic value of fluorescein angiography for studying retinal capillary detail. *Investig. Ophthalmol. Vis. Sci.* **2010**, *51*, 5864–5869. [[CrossRef](#)] [[PubMed](#)]
69. Damento, G.; Chen, M.H.; Leng, T. Spectral-Domain Optical Coherence Tomography Angiography of Central Retinal Artery Occlusion. *Ophthalmic Surg. Lasers Imaging Retina* **2016**, *47*, 467–470. [[CrossRef](#)]
70. Hautz, W.; Gołębiewska, J.; Czeszyk-Piotrowicz, A. Optical Coherence Tomography-Based Angiography in Retinal Artery Occlusion in Children. *Ophthalmic Res.* **2018**, *59*, 177–181. [[CrossRef](#)]
71. Ahn, S.J.; Park, K.H.; Ryoo, N.-K.; Hong, J.-H.; Jung, C.; Yoon, C.-H.; Han, M.-K.; Woo, S.J. No-Reflow Phenomenon in Central Retinal Artery Occlusion: Incidence, Risk Factors, and Clinical Implications. *PLoS ONE* **2015**, *10*, e0142852. [[CrossRef](#)]
72. Mendrinos, E.; Machinis, T.G.; Pournaras, C.J. Ocular Ischemic Syndrome. *Surv. Ophthalmol.* **2010**, *55*, 2–34. [[CrossRef](#)]
73. Brown, G.C.; Magargal, L.E. The ocular ischemic syndrome. *Int. Ophthalmol.* **1988**, *11*, 239–251. [[CrossRef](#)] [[PubMed](#)]
74. Sharma, S.; Ang, M.; Najjar, R.P.; Sng, C.; Cheung, C.Y.; Rukmini, A.V.; Schmetterer, L.; Milea, D. Optical coherence tomography angiography in acute non-arteritic anterior ischaemic optic neuropathy. *Br. J. Ophthalmol.* **2017**, *101*, 1045–1051. [[CrossRef](#)] [[PubMed](#)]
75. Lupidi, M.; Fiore, T.; Cerquaglia, A.; Coscas, G.; Cagini, C. Depth-Resolved Imaging of Papillary Vitreoretinal Neovascularization: OCT-Angiography Assessment in Ocular Ischemic Syndrome. *Retina (Phila. Pa.)* **2017**, *37*, e42–e44. [[CrossRef](#)] [[PubMed](#)]
76. Saito, K.; Akiyama, H.; Mukai, R. Alteration of optical coherence tomography angiography in a patient with ocular ischemic syndrome. *Retin. Cases Brief Rep.* **2019**. publish ahead of print. [[CrossRef](#)]
77. Mishra, A.; Luthra, S.; Baranwal, V.K.; Parihar, J.K.S. An interesting case of rubeosis iridis with neovascular glaucoma in a young patient. *Med. J. Armed Forces India* **2013**, *69*, 187–189. [[CrossRef](#)] [[PubMed](#)]

78. Ang, M.; Sim, D.A.; Keane, P.A.; Sng, C.C.A.; Egan, C.A.; Tufail, A.; Wilkins, M.R. Optical Coherence Tomography Angiography for Anterior Segment Vasculature Imaging. *Ophthalmology* **2015**, *122*, 1740–1747. [[CrossRef](#)] [[PubMed](#)]
79. Ang, M.; Cai, Y.; Tan, A.C.S. Swept Source Optical Coherence Tomography Angiography for Contact Lens-Related Corneal Vascularization. *J. Ophthalmol.* **2016**, *2016*. [[CrossRef](#)]
80. Ang, M.; Devarajan, K.; Das, S.; Stanzel, T.; Tan, A.; Girard, M.; Schmetterer, L.; Mehta, J.S. Comparison of anterior segment optical coherence tomography angiography systems for corneal vascularisation. *Br. J. Ophthalmol.* **2018**, *102*, 873–877. [[CrossRef](#)]
81. Ang, M.; Cai, Y.; Shahipasand, S.; Sim, D.A.; Keane, P.A.; Sng, C.C.A.; Egan, C.A.; Tufail, A.; Wilkins, M.R. En face optical coherence tomography angiography for corneal neovascularisation. *Br. J. Ophthalmol.* **2016**, *100*, 616–621. [[CrossRef](#)]
82. Cai, Y.; Alio Del Barrio, J.L.; Wilkins, M.R.; Ang, M. Serial optical coherence tomography angiography for corneal vascularization. *Graefes Arch. Clin. Exp. Ophthalmol. Albrecht Von Graefes Arch. Klin. Exp. Ophthalmol.* **2017**, *255*, 135–139. [[CrossRef](#)]
83. Brunner, M.; Romano, V.; Steger, B.; Vinciguerra, R.; Lawman, S.; Williams, B.; Hicks, N.; Czanner, G.; Zheng, Y.; Willoughby, C.E.; et al. Imaging of Corneal Neovascularization: Optical Coherence Tomography Angiography and Fluorescence Angiography. *Investig. Ophthalmol. Vis. Sci.* **2018**, *59*, 1263–1269. [[CrossRef](#)] [[PubMed](#)]
84. Liu, Y.-C.; Devarajan, K.; Tan, T.-E.; Ang, M.; Mehta, J.S. Optical Coherence Tomography Angiography for Evaluation of Reperfusion following Pterygium Surgery. *Am. J. Ophthalmol.* **2019**. [[CrossRef](#)] [[PubMed](#)]
85. Ang, M.; Cai, Y.; MacPhee, B.; Sim, D.A.; Keane, P.A.; Sng, C.C.A.; Egan, C.A.; Tufail, A.; Larkin, D.F.; Wilkins, M.R. Optical coherence tomography angiography and indocyanine green angiography for corneal vascularisation. *Br. J. Ophthalmol.* **2016**, *100*, 1557–1563. [[CrossRef](#)] [[PubMed](#)]
86. Pellegrini, M.; Cozzi, M.; Staurengi, G.; Corvi, F. Comparison of wide field optical coherence tomography angiography with extended field imaging and fluorescein angiography in retinal vascular disorders. *PLoS ONE* **2019**, *14*, e0214892. [[CrossRef](#)] [[PubMed](#)]
87. Spaide, R.F.; Fujimoto, J.G.; Waheed, N.K. Image artifacts in optical coherence tomography angiography. *Retina (Phila. Pa.)* **2015**, *35*, 2163–2180. [[CrossRef](#)] [[PubMed](#)]
88. Adabi, S.; Conforto, S.; Clayton, A.; Podoleanu, A.G.; Hojjat, A.; Avanaki, M.R.N. An intelligent speckle reduction algorithm for optical coherence tomography images. In Proceedings of the 4th International Conference on Photonics, Optics and Laser Technology (PHOTOPTICS), Rome, Italy, 27–29 February 2016; pp. 1–6.
89. Avanaki, M.R.N.; Cernat, R.; Tadrous, P.J.; Tatla, T.; Podoleanu, A.G.; Hojjatoleslami, S.A. Spatial Compounding Algorithm for Speckle Reduction of Dynamic Focus OCT Images. *IEEE Photonics Technol. Lett.* **2013**, *25*, 1439–1442. [[CrossRef](#)]
90. Wang, L.; Li, Y.; Li, Y.; Li, K. Improved speckle contrast optical coherence tomography angiography. *Am. J. Transl. Res.* **2018**, *10*, 3025–3035.
91. Corvi, F.; Pellegrini, M.; Erba, S.; Cozzi, M.; Staurengi, G.; Giani, A. Reproducibility of Vessel Density, Fractal Dimension, and Foveal Avascular Zone Using 7 Different Optical Coherence Tomography Angiography Devices. *Am. J. Ophthalmol.* **2018**, *186*, 25–31. [[CrossRef](#)]

